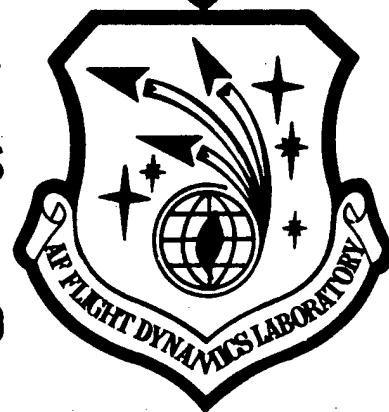


**AIR FORCE FLIGHT DYNAMICS LABORATORY
DIRECTOR OF LABORATORIES
AIR FORCE SYSTEMS COMMAND
WRIGHT PATTERSON AIR FORCE BASE OHIO**



**CORRELATION OF HEAT TRANSFER DATA OBTAINED BY THE
INFRARED SCANNER AND TEMPERATURE SENSITIVE COATING TECHNIQUES**

Max E. HILLSAMER

February 1975

**Project Number 1426
Task Number 142601**

Approved for public release; distribution unlimited

**High Speed Aero Performance Branch
Flight Mechanics Division
Air Force Flight Dynamics Laboratory**


**Reproduced From
Best Available Copy**

20000509 146

FOREWORD

This report summarizes data taken in interfering flow field tests conducted in the Air Force Flight Dynamics Laboratory's High Temperature Facility during August 1974 using an infrared scanning system. The effort was conducted under Project Nr. 1426, "Aerodynamic Ground Test Techniques", Work Effort Nr. 14260116, "Infrared Scanning Systems Techniques". The tests were conducted in-house as a joint effort of the High Speed Aeroperformance Branch (FXG) and the Experimental Engineering Branch (FXN) of the Flight Mechanics Division. Mr. Edward L. White, AFFDL/FXN was the principal investigator.

This technical report has been reviewed and is approved.


PHILIP P. ANTONATOS
Chief, Flight Mechanics Division
AF Flight Dynamics Laboratory

ABSTRACT

An infrared scanning system was used to measure heat transfer rates on a sharp leading edge flat plate with a three-dimensional shock generator attached. Results were compared with data previously obtained on the same model using temperature sensitive phase change coatings. The tests were conducted in the Air Force Flight Dynamics Laboratory's High Temperature Facility (HTF) at a Mach number of 10, stagnation pressure of 300 psia, and stagnation temperature of 2200 deg R. The corresponding Reynolds number was approximately 2.8×10^5 per foot.

Results indicate that the IR scanner method of obtaining heat transfer coefficients compares quite favorably with the temperature sensitive coating method, however; data quality was degraded when the scanner viewing angle was other than normal to the model surface.

TABLE OF CONTENTS

Section		Page
I	Introduction	1
II	Apparatus	3
	A. Model	3
	B. Wind Tunnel	3
	C. Instrumentation	4
III	Test Description	5
	A. Test Conditions	5
	B. Test Procedure	5
	C. Data Reduction	5
IV	Results	9
V	Conclusions	14
	References	15
	Tables	
I	Wind Tunnel Test Log	16

ILLUSTRATIONS

Figure	Title	Page
1	Shock Generator Model Planform	17
2	Solution of One-Dimensional Semi-Infinite Slab Heat Conduction Equation Using Teflon Thermal Properties. $\sqrt{\rho c k} = 0.0367 \text{ Btu/ft}^2 \text{ sec}^{1/2} \text{ }^\circ\text{F}$	18
3	Representative Temperature/Time Histories	19
4	Heat Transfer Coefficients for Several Times on Run 199	
	a. Y = 1.42 in.	20
	b. Y = 2.33 in.	21
	c. Y = 3.24 in.	22
5	Comparison of Heat Transfer Coefficients for $X_F = 0 \text{ in.}$, Scan Angle = 0 deg	
	a. Y = 1.42 in.	23
	b. Y = 2.33 in.	24
	c. Y = 3.24 in.	25
6	Comparison of Heat Transfer Coefficients for $X_F = 8 \text{ in.}$, Scan Angle = 0 deg.	
	a. Y = 1.42 in.	26
	b. Y = 2.33 in.	27
7	Comparison of Heat Transfer Coefficients for $X_F = 0 \text{ in.}$, Scan Angle = - 10 deg	
	a. Y = 1.42 in.	28
	b. Y = 2.33 in.	29
	c. Y = 3.24 in.	30
8	Comparison of Heat Transfer Coefficients for $X_F = 0 \text{ in.}$, Scan Angle = - 20 deg.	
	a. Y = 1.42 in.	31
	b. Y = 2.33 in.	32
	c. Y = 3.24 in.	33
9	Distribution of Heat Transfer Coefficients	
	a. Reference 7, Run 297	34
	b. IR Scanner Run 199	35
10	Isometric Mapping of Heat Transfer Coefficients for IR Run 199	

SYMBOLS

c	Specific heat, Btu/lb - °F
erfc	Complementary error function
h	Heat Transfer coefficient, Btu/ft ² -sec-°R
k	Thermal conductivity, Btu/sec-ft-°R
L	Slab thickness, ft
M	Mach number
r	Recovery factor
T	Temperature, °R or °F
t	time, sec
\bar{T}	$(T_{pc} - T_i) / (T_{aw} - T_i)$
X	Distance from model leading edge, in. or ft.
Y	Distance from right edge of Teflon insert, in. or ft
y	Normal distance from surface of slab, ft
α	Thermal diffusivity, k/ ρc , ft ² /sec
β	Semi-infinite slab parameter, $h \sqrt{t} / \sqrt{\rho c k}$
γ	Ratio of specific heats
δ	Fin deflection angle, deg
λ	Dummy variable of integration
ρ	Density, lb/ft ³
Subscripts	
aw	Adiabatic wall
d	Thermal diffusion
i	Initial
pc	Phase change
∞	Freestream

INTRODUCTION

While various methods are available for the measurement of aerodynamic heat transfer rates in high speed wind tunnels; each method has disadvantages either in model construction or data acquisition techniques. Metallic models equipped with thermocouple are costly to build, and instrumentation can only be provided at selected points. Temperature sensitive coatings, such as presented in References 1 and 2, can provide total coverage of an aerodynamic model, but old coatings must be removed and new ones applied for each test run. Models coated with encapsulated liquid crystals have been tested at Mach numbers to 3.0 with the coatings being cycled through their temperature ranges many times (Ref. 3). However, the available liquid crystal temperature range is presently too low for use at elevated (2300°R) temperatures.

An infrared scanner (IR) system has been developed by the Lockheed-California Company for use in the AFFDL High Temperature Facility (HTF) to measure heating rates on wind tunnel models. The system was designed for high speed scanning of the model with a total of 810 temperatures being measured during each scan. Nonmetallic models of low thermal conductivity and surface emissivity values near 1.0 are used. Reference 4 presents a complete description of the IR scanning system and some of the early developmental results obtained from it.

Evaluation tests of the IR scanning system were conducted in the HTF in August 1974 using a model which was previously employed in the experimental work of Reference 2. Wind tunnel conditions were the same for both tests so that IR scanner data could be compared with previously obtained results.

The purpose of this report is to present the data reduction techniques used and to compare experimental results obtained on the same wind tunnel model using the IR scanning system and the temperature sensitive phase change coating technique. The reader is referred to reference 4 for a more complete description of the scanner system.

II. APPARATUS

A. Model

The model used during the current test was fabricated by Lockheed Missiles and Space Company for use during temperature sensitive paint tests. The model was a flat plate 8 inches wide, 16 inches long and 1.25 inches thick with a leading edge bevel angle of 20 degrees. The top surface was recessed 0.375 in. starting at a station 2 in. aft of the leading edge to permit installation of instrumented inserts. For the IR scanner test, the insert used was 0.25 in. thick teflon sheet backed by a stainless steel sheet. The teflon surface to be scanned was painted with 3M "Nextel" velvet coating ¹⁰¹ (100-C10 black) to produce a spectral emissivity of approximately 0.92.

A stainless steel shock generator fin 6 in high and 0.50 in. thick with 20 deg leading edge bevel was mounted on the right side of the model perpendicular to the scanned surface. Positioning of the fin to change shock deflection angle and axial location was accomplished through the use of different mounting brackets.

A hollow 1.25 in. dia. sting allowed direct mounting of the model to the injection strut without the use of adapters. Figure 1 shows a schematic of the model used.

B. Wind Tunnel

The test was performed in the AFFDL High Temperature Facility (HTF) which is completely described in Ref. 5 and 6. The facility is a hypersonic blowdown wind tunnel utilizing an alumina pebble bed heater as its heat source. For this test, a contoured Mach 10 nozzle with a 24 in. exit diameter was installed. The facility can be operated at stagnation pressures from 100 to 600 psia and stagnation temperatures up to 3500°R.

C. Instrumentation

All model temperatures were measured with the IR scanner system. The system was orientated to scan a 6 in. x 15 in. section of the model 5 times per second. Each scan consisted of 18 rows by 45 points per row for a total of 810 temperature points. Signals from the IR scanner were sent through an Electronic Engineering Co., Model 761A1 analog-to-digital converter of the IR system and stored on magnetic tape. ^{BY THE CDC 160A.} Data reduction from ^{THE THREE BINARY CODED} ~~raw voltages~~ to ^{DECIMALS FORMAT} temperatures was accomplished on the CDC-160A computer. Temperatures were printed out in an 18x45 matrix array in the same position the scanner sampled them.

III. TEST DESCRIPTION

A. Test Conditions

In order to compare IR scanner data directly with temperature sensitive phase change paint data, test conditions run on the previous temperature sensitive paint test (Ref 2) were repeated for this test. Reservoir stagnation pressure was nominally 300 psia, and stagnation temperature approximately 2200°R. Table 1 lists the conditions actually achieved during each run.

B. Test Procedure

Before the first test run each day, the pebble bed heater was evacuated to less than 30 mm Hg to remove moisture from the pebbles. The moisture is formed as a product of combustion of the propane/air/oxygen mixture used to heat the pebbles.

During a data run the wind tunnel was started and brought to the desired conditions. Reservoir pressure and temperature and test section impact pressure were recorded before injection of the model. ^{AND DURING THE MODEL TEST,} A switch on the model injection strut started the IR scanner data system when the model reached tunnel centerline. The model was left in the flow for approximately 5 sec. then retracted, and the wind tunnel was shut down. A second model injection was attempted on two of the runs, but the model surface was too hot in spots to obtain meaningful data.

C. Data Reduction

Heat transfer coefficients were calculated by the method used in Ref. 2 for a one-dimensional semi-infinite slab. As in Reference 2 the primary assumptions are (1) the depth of heat penetration into the model is small

compared with the wall thickness so that the model acts like a semi-infinite slab; (2) the model is initially isothermal; (3) the surface is subjected to an instantaneous step in aerodynamic heating at time zero and the heat transfer coefficient does not vary with time; and (4) the model thermal conductivity, density and specific heat do not vary with temperature.

Data reduction by the semi-infinite slab method as used in Refs. 1 and 2 consisted of measuring the test time required for a point on the model surface to reach a known temperature, as indicated by the coating melt patterns, and calculating the corresponding heat transfer coefficient by the solution of the one-dimensional transient heat conduction equation:

$$\frac{\partial T}{\partial t} = \frac{k}{\rho c} \frac{\partial^2 T}{\partial y^2} \quad (1)$$

Boundary conditions used which best describe the actual wind tunnel test are:

$$T(y, 0) = T_i$$

$$T(\infty, t) = T_i$$

$$\frac{\partial T(0, t)}{\partial y} = \frac{h}{k} [T_{AW} - T(0, t)]$$

The solution of Equation (1) with stated boundary conditions and assumptions is

$$\bar{T} \equiv \frac{T_{pc} - T_i}{T_{AW} - T_i} = 1 - e^{\beta^2} \operatorname{erfc} \beta \quad (2)$$

where

$$\beta \equiv \frac{h\sqrt{\alpha t}}{k} = \frac{h\sqrt{t}}{\sqrt{eck}}$$

$$T_{AW} = \left[\frac{1 + \frac{\gamma-1}{2} r M_{\infty}^2}{1 + \frac{\gamma-1}{2} M_{\infty}^2} \right] T_0$$

For semi-infinite slab theory to be applicable, the time required for the phase change to occur must be small compared to the thermal diffusion time of the model wall. The thermal diffusion time is approximated by the equation (Ref. 1):

$$t_d \approx \frac{0.2L^2}{\alpha} \approx \frac{0.2L^2 ec}{k} \quad (3)$$

Thermal diffusion time for the 0.25 in. thick teflon model surface was calculated at about 67 sec.

For the temperature sensitive paint tests of Ref. 2, Equation (2) was used to derive the curves of Fig. 2 for TFE Teflon thermal properties of $\sqrt{eck} = 0.0367 \text{ B/ft}^2\text{-sec}^{1/2}\text{-}^\circ\text{R}$ so the heat transfer coefficient could be obtained directly as a function of \bar{T} and melt time. The initial temperature of the model was assumed to be 80°F and T_{pc} was the known coating melt temperature, so for each run \bar{T} was constant for all points on the model surface. Melt times were determined from timed sequence photographs of the model in the tunnel airflow, and were variable at different sections of the model. With \bar{T} and melt times known, heat transfer coefficients were then obtained from Fig. 2.

Reduction of the IR scanner data was basically the same as for the temperature sensitive paint test. However, T_{pc} was replaced by model surface temperature, T_M , to determine \bar{T} . Instead of a coating melt time, a data

reduction time was determined from temperature-time histories at several points on the model. For each run, heat transfer coefficients were obtained at a constant time but with variable \bar{T} for each scan location. All runs were reduced at approximately 4.5 sec after the model was injected to assure that any model vibrations induced by the injection system were damped out and flow had properly established.

IV. RESULTS

A minimum of 2 runs were made at each model attitude tested in order to check the repeatability of the IR scanner system. Because of the large number of temperatures measured in each scan (810), heat transfer coefficients were not calculated at each point on the model. Data presented in this report are sufficient to show the correlation obtained between the temperature sensitive paint method and the IR scanner method.

Temperature-time histories of 6 model points on each of three runs are shown in figure 3. Number designations of the symbols refer to row/point locations of the model temperatures. At times under 2 sec, temperatures were scattered and no meaningful slopes could be obtained. The timer for the IR scanner data recording system was actually activated before the model reached the tunnel centerline, and flow was not stable for the first 2 sec of data. Retraction of the model was started after about 5 sec of data recording, and temperatures after start of model retraction were not useable.

Heat transfer coefficients were calculated for 5 times from 2.15 to 5.35 sec along 3 rows on Run 199. These data, presented in Fig. 4 (a-c), show lower heat transfer coefficients in the fin induced high heating region at 2.15 and 2.95 sec than at the later reduction times. Coefficients at the reduction times of 3.75, 4.55 and 5.35 sec are very nearly equal in magnitude on each row presented. From the temperature-time histories of Fig. 3 and the heat transfer coefficients of Fig. 4, it was decided that the optimum data reduction time would be between 3.5 and 5 sec after the start of the IR scanner. The remainder of the data presented in this report were calculated at approximately 4.5 sec, or the 16th frame of the IR scanner data.

↓
3.2 SEC ?

↓
22.5 FRAMES ?

Temperature sensitive paint results presented in this report were obtained from Ref. 2 and 7. Temperature sensitive paint data previously obtained on the Teflon models was shown in Reference 7 to have a degree of uncertainty for two reasons. (1) Extreme difficulty in accurately determining paint melt lines on the model was caused by the lack of contrast between the light pastel green color of the paint and the white model surface. (2) There was also a noted discontinuity in the specific heat for Teflon in the temperature range below ^{90°F} 100°F. For these reasons some disagreement between Ref. 7 and IR scanner results is anticipated.

The two main objectives of this test program were to compare heat transfer coefficients in a high heating region obtained by the IR scanner system with results obtained from temperature sensitive coatings, and to investigate the effect of IR scanner viewing angle on the resultant data.

Figures 5 through 8 present comparisons of the results obtained using the two different techniques. Three rows of data, at Y=1.42, 2.33 and 3.24 in. from the right side of the model are presented. Little influence of the shock generator fin was evident at lateral distances greater than 3.24 in., and the three rows shown present the best available data for comparisons of the two methods.

Figures 5 and 6 present results with the IR scanner viewing angle at 0 deg, or directly normal to the model surface. This orientation was used as the reference point. The scanner was then moved forward and angled back to produce viewing angles of -10 and -20 deg with the reference point. Results of changing viewing angle to the two different values are shown in Figs. 7 and 8, respectively.

Heat transfer coefficients shown in Fig. 5 indicate that reasonable agreement existed between the data of Ref. 7 and the IR scanner results with the exception of $Y = 1.42$ in. (Fig 5a). The IR data indicates the heating peak occurs approximately 1 in. ahead of the peak shown in Ref. 7 data. Inaccuracies of this type in measuring the location of peak heating for both methods accounts for much of the disagreement between the data sets. Also, as the IR scanner sweeps along the model, the viewing angle is changed. The viewing angle between the peak heating point and scanner reference point was calculated as 6.6 deg for Fig. 5a. Higher heat transfer coefficients for Run 200 than for Run 199 were caused by assuming an initial isothermal temperature of 90°F on the model for both runs. First data frames for each run showed that the initial temperatures for Run 200 were approximately 5 deg higher than for Run 199. Also, the model surface was also not completely isothermal at the start of Run 200 because of residual heat from previous running.

Figure 6 shows a comparison of IR scanner and Ref. 7 results with the shock generator fin 8 in. aft of the model leading edge and deflected 10 deg. Poor agreement between the two methods is evident both in location and magnitude of the data in the peak heating region. Scanner viewing angle between the reference point and the indicated point of peak heating was calculated for Fig. 6a as 9.1 deg, indicating a possible viewing angle effect in this data.

Results of moving the IR scanner to produce a viewing angle of -10 deg with the model reference point is shown in Figure 7. Generally poor correlation between the two methods is shown in these data, both in location and magnitude of the peak heating regions. While IR scanner runs 212 and 213 agree quite well with each other, peak heating regions defined by these data are aft of the Ref. 7 peak heating regions.

Figure 8 compares IR scanner results with Ref 7 results for the IR scanner viewing angle changed to -20 deg. Poor agreement is seen between the IR scanner data and Ref. 7, and even the two IR scanner runs are not in agreement with each other. The best correlation is seen in Fig. 8b ($Y=2.33$), where interference heating peaks are evident in the IR scanner data. At $Y=1.42$ in. and 3.24 in. no easily defineable interference heating peaks are observed.

From the results presented in Fig. 5-8 it is apparent that, although there are errors and uncertainties in Ref 7 data caused by difficulties in accurately determining paint melt lines, scanner viewing angle consistently contributes to disagreements between the two methods. With the IR scanner positioned directly over the center of the model, it is felt that results obtained from the IR scanner method are as reliable as results obtained from the temperature sensitive paint studies.

Figure 9 (a-b) shows lines of constant heat transfer coefficients in the interference region of the model surface. While the temperature sensitive coating technique (Fig. 9a) indicates one long area of peak heating ($h = .00143 \text{ b/ft}^2 \text{ sec}^\circ \text{R}$), the IR scanner results indicate two areas in the interference band. Results presented in Ref. 2 (Fig. 48) are a compilation from several runs and do indicate the secondary area of peak heating. There is speculation in Ref. 2 that this second peak may be a result of boundary layer transition in the interaction region.

A disadvantage of the use of the temperature sensitive coating method is the necessity of using only one melt temperature coating on each run. Reference 7 data presented in this report were obtained using paint with a melt temperature of 150°F , which was satisfactory in the regions of highest

heating but was unsuitable for overall mapping of the model surface.
Complete mapping of a 5.7 in x 14.6 in. section of the model surface was possible through the use of the IR scanner. Figure 10 presents a representative diagram of the results obtainable from the IR scanner. Where only the peak interference heating region was defined in the temperature sensitive paint data, a secondary heating region is shown in the IR scanner data of Fig. 10. This secondary region occurs in the approximate location where the bow shock from the fin intersects with the model surface. Results shown in Fig. 10 are supported by the oil flow findings and the interaction region heating distributions presented in Ref. 2 (Fig. 41 and 48 respectively).

V. CONCLUSIONS

The IR scanning system has been shown to provide a useful method of obtaining heat transfer coefficients on the surface of the flat plate interference heating model. Considering the problems encountered in obtaining heating rates from the comparable temperature sensitive coating method, the quality of the IR scanner results is considered as good as that of Refs. 2 and 7 results. A broader range of heating rates can be measured by the IR scanner, and model surfaces do not have to be prepared before each run.

It was shown that scanner viewing angle does affect quality of the IR scanner data, and best results were obtained with the scanner normal to the mid point of the model. No attempt was made to use the IR scanner to obtain heating rates on a non-planar model. With scanner viewing angle affecting data as it does, it is felt that the IR scanner would be unsuitable at present for use with a non-planar model. Future studies will investigate this problem more closely and incorporate view angle correction factors into a data reduction program.

REFERENCES

1. Jones, R.A. & Hunt, J.L., Use of Fusible Temperature Indicators for Obtaining Quantitative Aerodynamic Heat-Transfer Data, NASA TR R-230, February 1966.
2. Schultz, H.D., Experimental and Analytical Investigation of Temperature Sensitive Paints, AFFDL-TR-72-52, June 1972.
3. Hillsamer, Max E., Low Mach Number Temperature Measurements Using Encapsulated Liquid Crystals, AFFDL-TM-73-120-FXG, August 1973.
4. White, Edward L., Development of an Infrared Scanning System for the Empirical Evaluation of Aerodynamic Heating, Paper #51 presented at 5th Symposium on Temperature, Washington, D.C. 21-24 June 1971.
5. Czysz, P., "The High Temperature Hypersonic Gasdynamic Facility Estimated Mach 6 through 14 Performance", ASD-TDR-63-456, June 1963.
6. Schnabel, C., Smith, R.R., and Dahlem V., "Performance Estimates for the AFFDL Pebble Bed Heated Hypersonic Wind Tunnel", FXG TM 67-3, July 1967.
7. Schultz, H.D., "Pressure and Heat Transfer Measurements in Regions of Three-Dimensional Shockwave-Boundary Layer Interactions", LMSC-D157341, 20 March 1972.

TABLE 1. WIND TUNNEL TEST LOG

RUN NR.	DATE	P ₀ PSIA	T ₀ °R	X _F IN.	SCAN ANGLE DEG.	REMARKS	FRAME NR 1 ISOTHERMAL
199	160874	301.3	2329	0	0		NO
200		303.0	2325	0	0		NO
201		297.7	2311	0	0	2 INJECTIONS	NO
202	190874	302.3	2314	8	0		YES
203		300.3	2283	8	0		RT. REAR CORNER HOTTER
204		299.7	2271	8	0	2 INJECTIONS	EXTREME RT. REAR CORNER HOTTER
205	200874	301.3	2251	NO FIN	0		YES
206		299.0	2244	NO FIN	0		RIGHT REAR CORNER COOLER
207		301.0	2210	NO FIN	-10	2 INJECTIONS	RIGHT REAR CORNER COOLER
208		299.0	2233	NO FIN	-10		RIGHT REAR CORNER COOLER
209		298.4	2228	NO FIN	-20	20 AUG 74 1410 HRS	RIGHT REAR CORNER COOLER
210		300.3	2191	0	-20	20 AUG 74 1500 HRS	NO
211	210874	301.0	2205	0	-20	21 AUG 74 1300 HRS	NO
212		296.4	2180	0	-10	21 AUG 74 1045 HRS	NO
213		302.6	2249	0	-10	21 AUG 74 1335 HRS	NO
NOTES:							

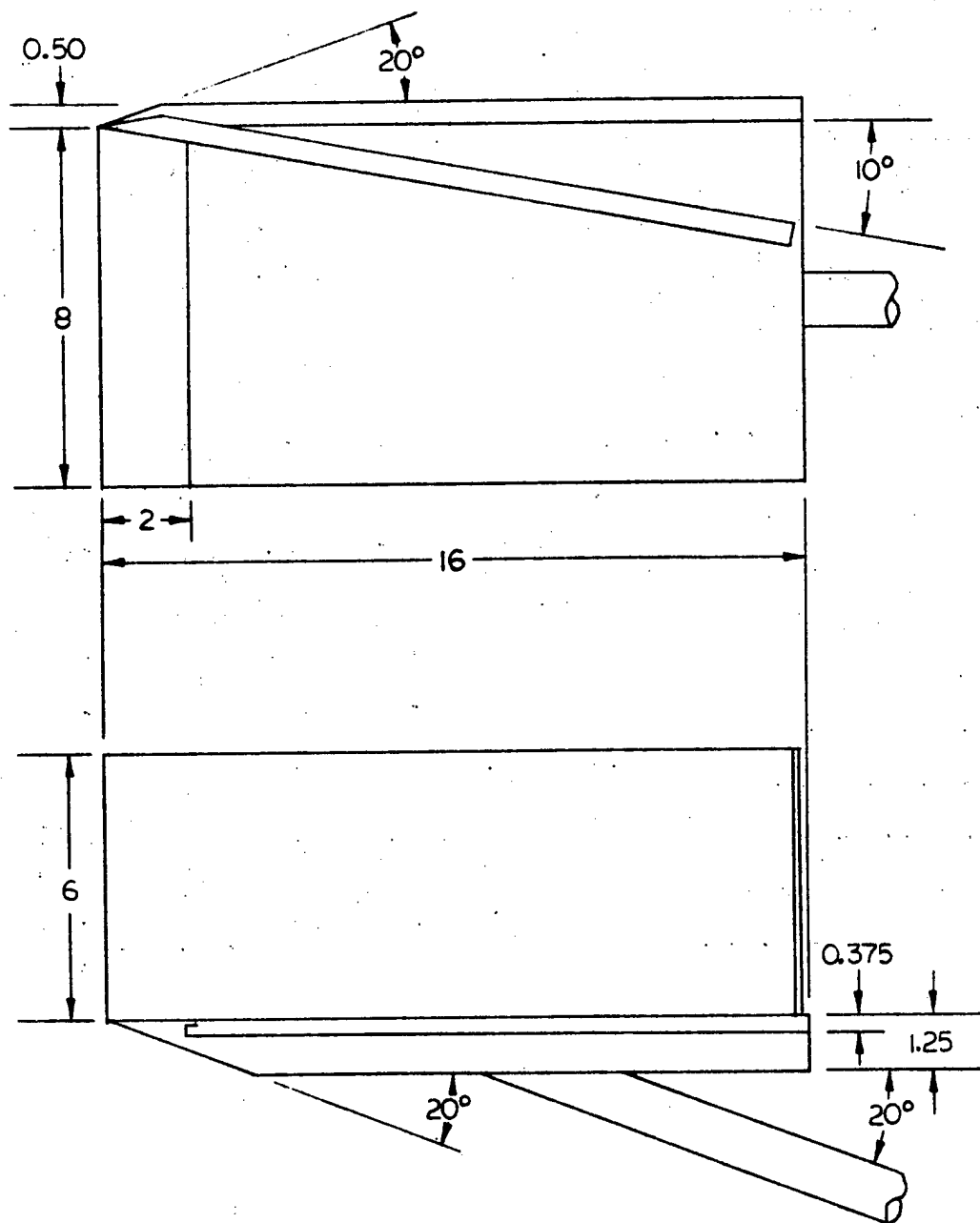


Figure 1. Shock Generator Model Planform

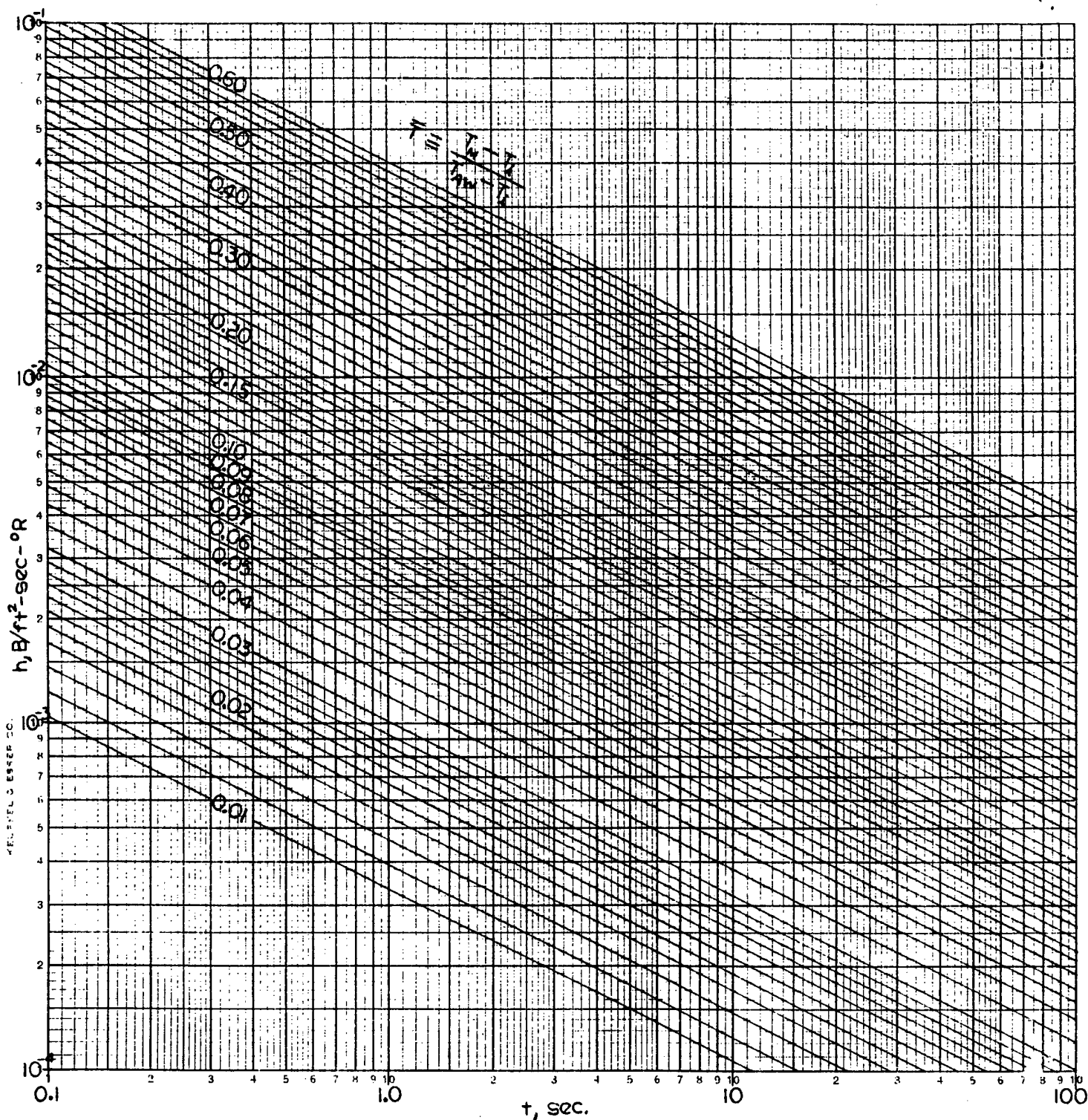


Figure 2. Solution of one-Dimensional Semi-Infinite Slab
Heat Conduction Equation Using Teflon Thermal
Properties $\sqrt{pck} = 0.0367 \text{ Btu/ft}^2 \text{sec}^{1/2} \text{ } ^\circ\text{F}$

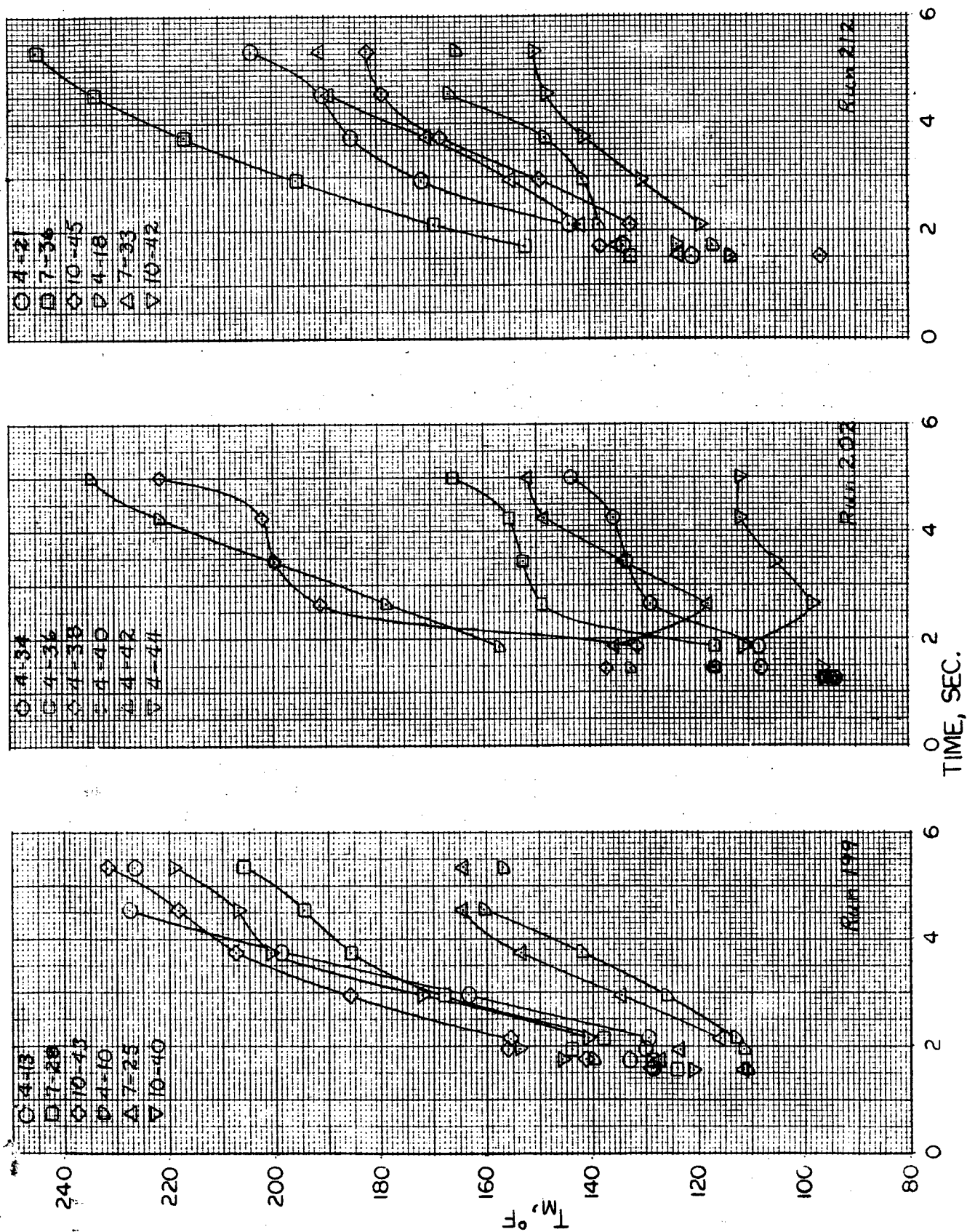


Figure 3. Representative Temperature/Time Histories

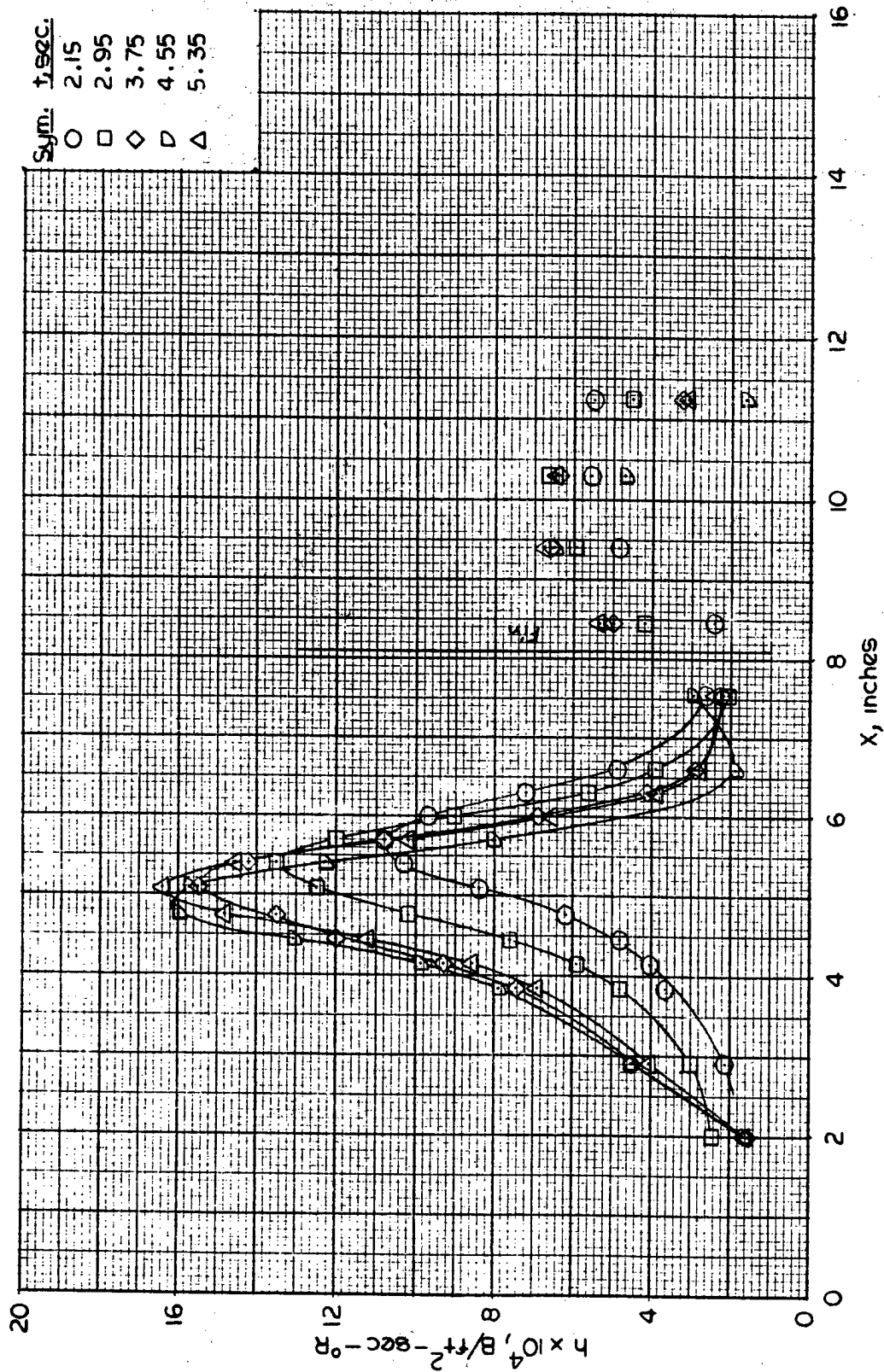
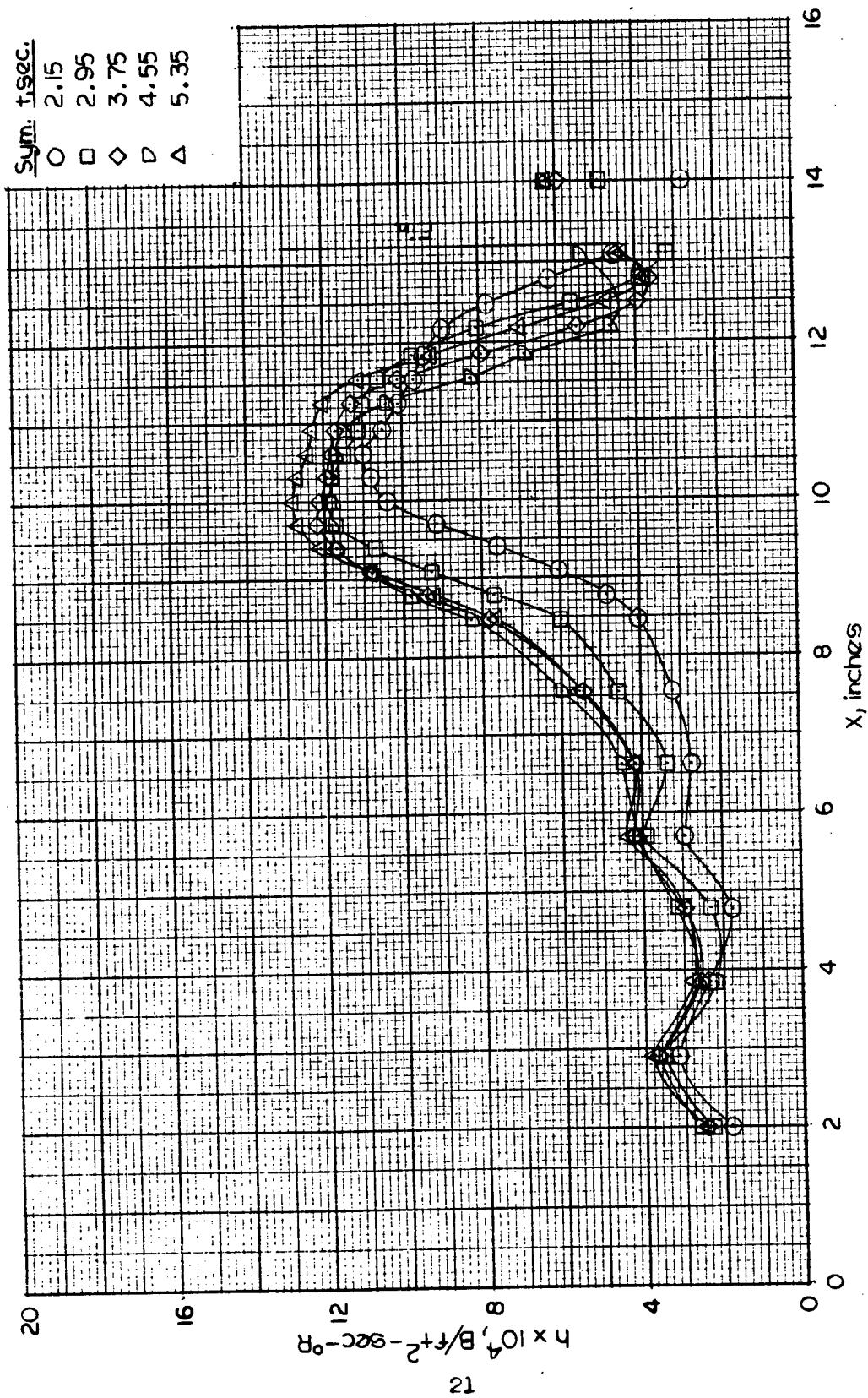
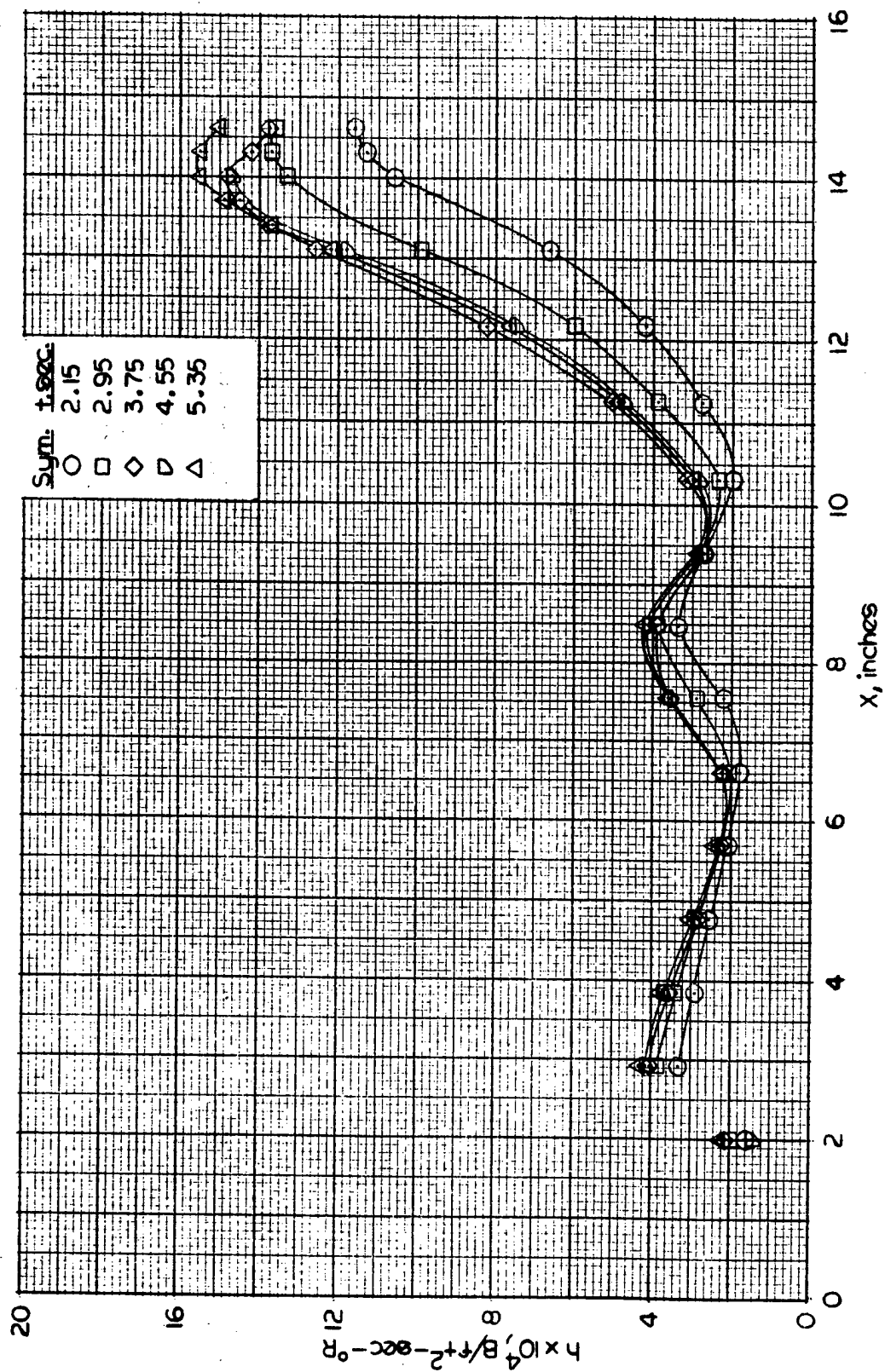


Figure 4. Heat Transfer Coefficients for Several Times on Run 199



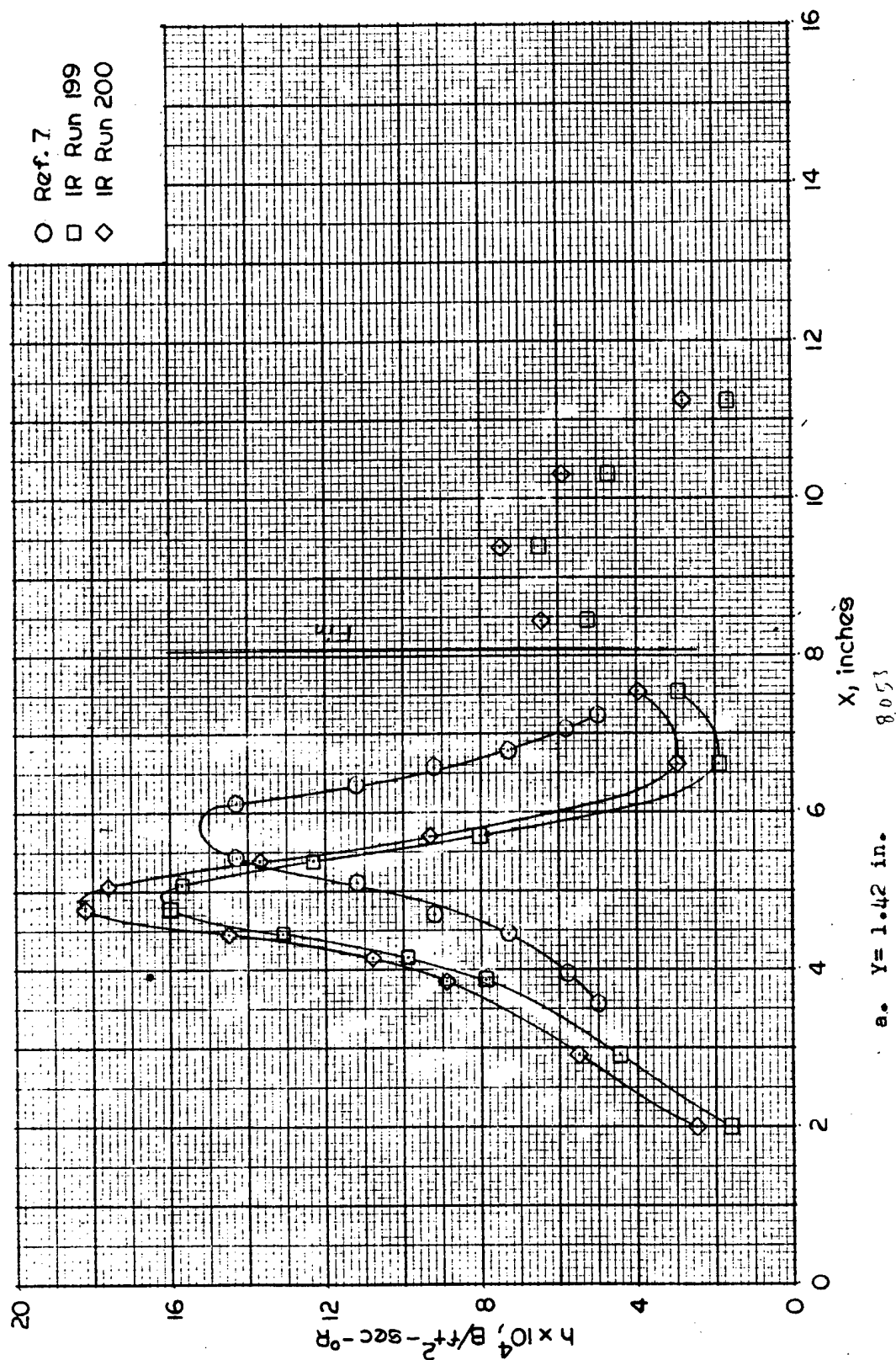
b. $Y = 2.33$ in

Figure 4. (Continued)



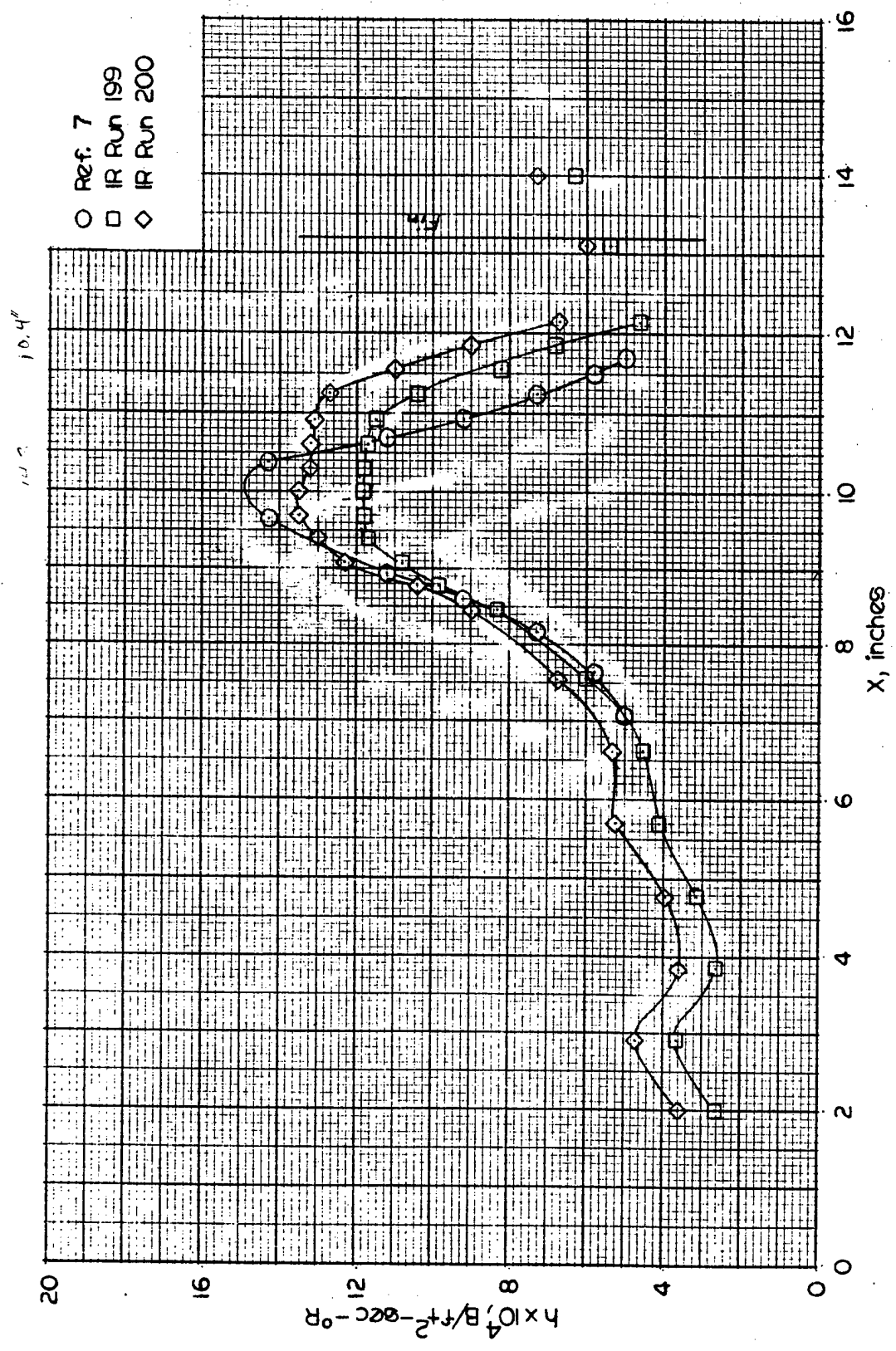
c. $Y = 3.24 \text{ in.}$

Figure 4. (concluded)



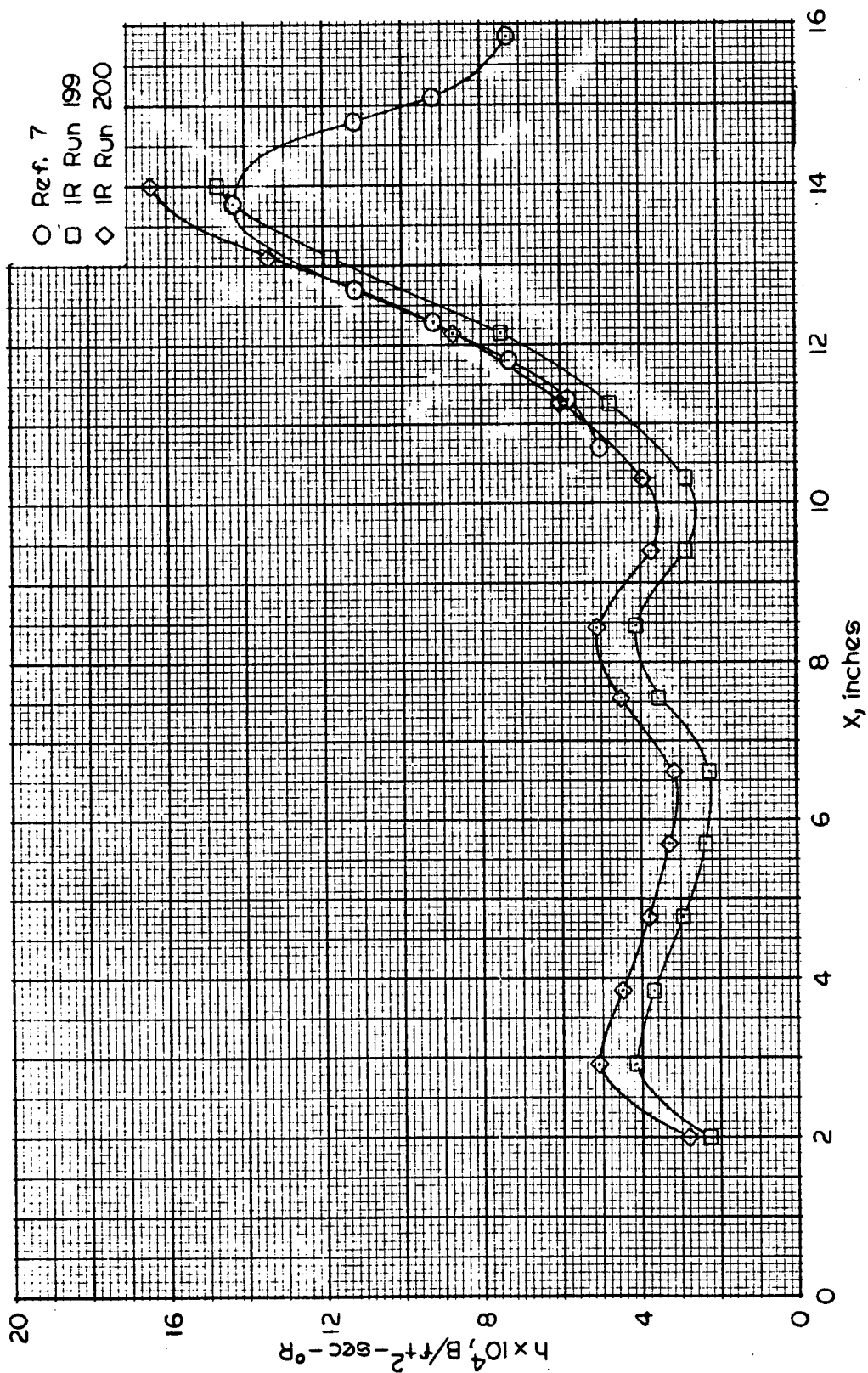
a. $Y = 1.42$ in. 8.053

Figure 5. Comparison of heat Transfer Coefficients for $\lambda_F = 0$ in., Scan Angle = 0 deg.



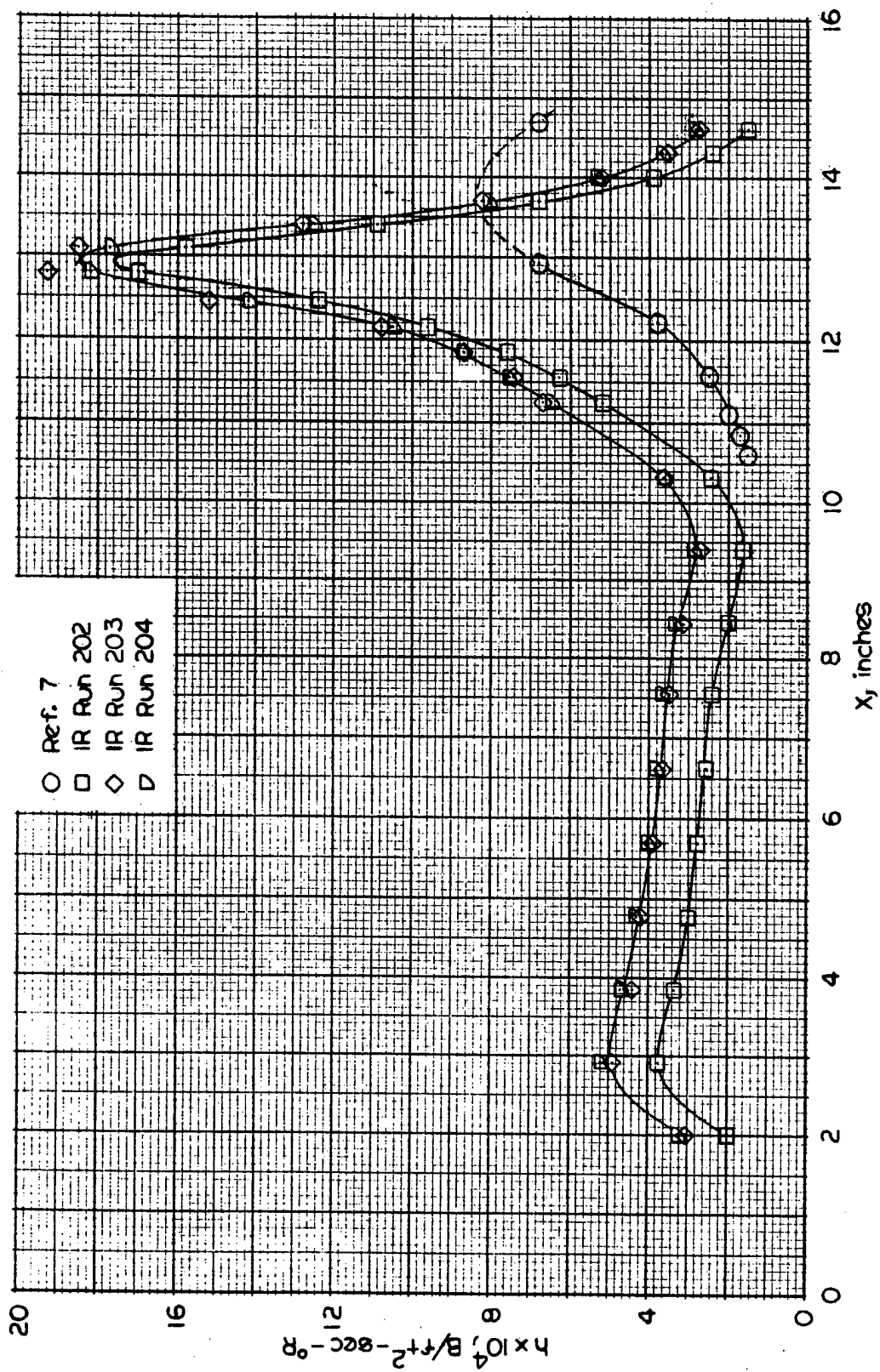
b. $Y = 2.33$ in.

Figure 5. (Continued)



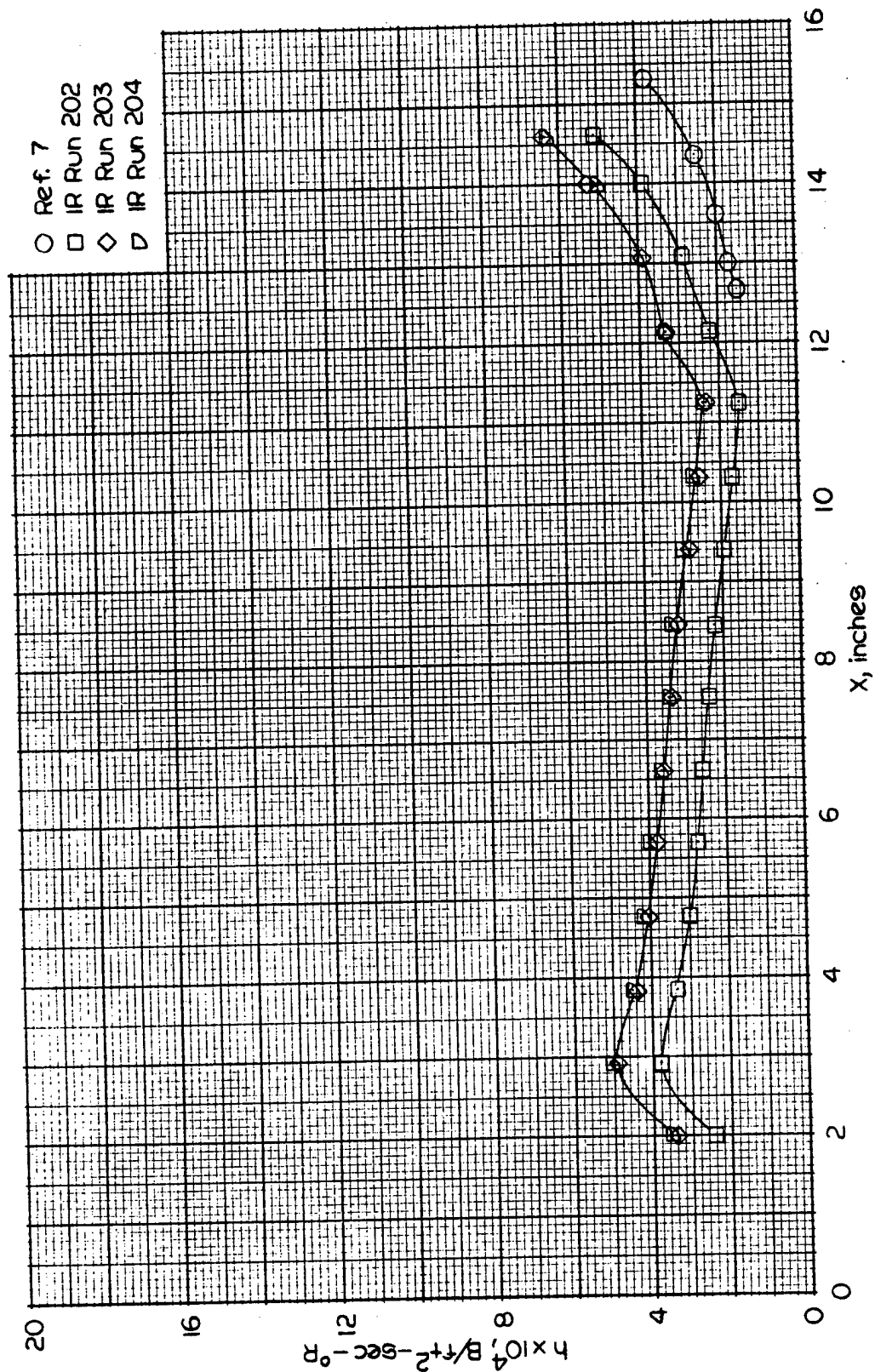
c. $Y = 3.24$ in.

Figure 5. (concluded)



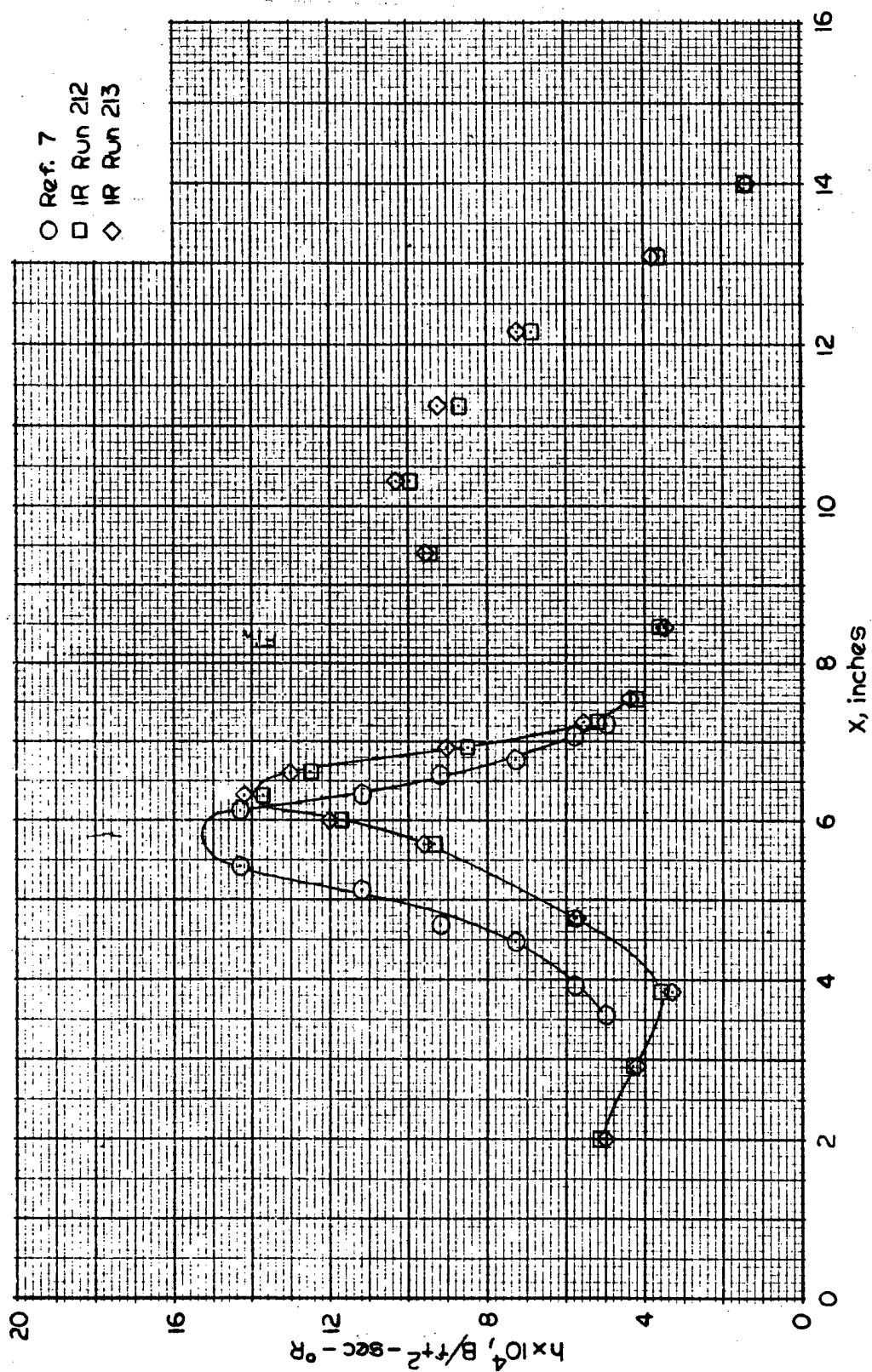
a. Y = 1.42 in.

Figure 6. Comparison of Heat Transfer Coefficients for $X_F = 8$ in., Scan Angle = 0 deg.



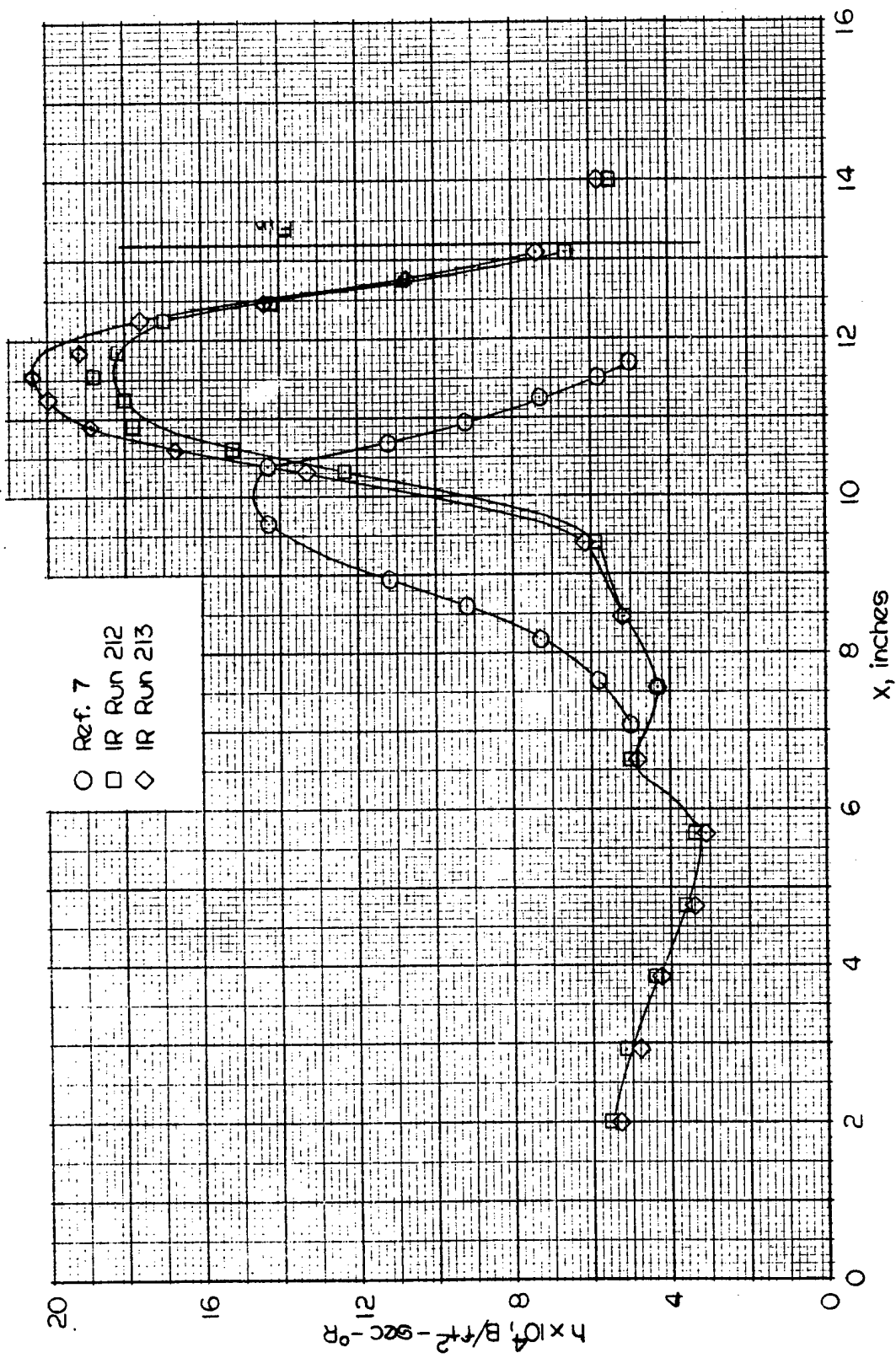
b. $Y = 2.33$ in.

Figure 6. (Concluded)



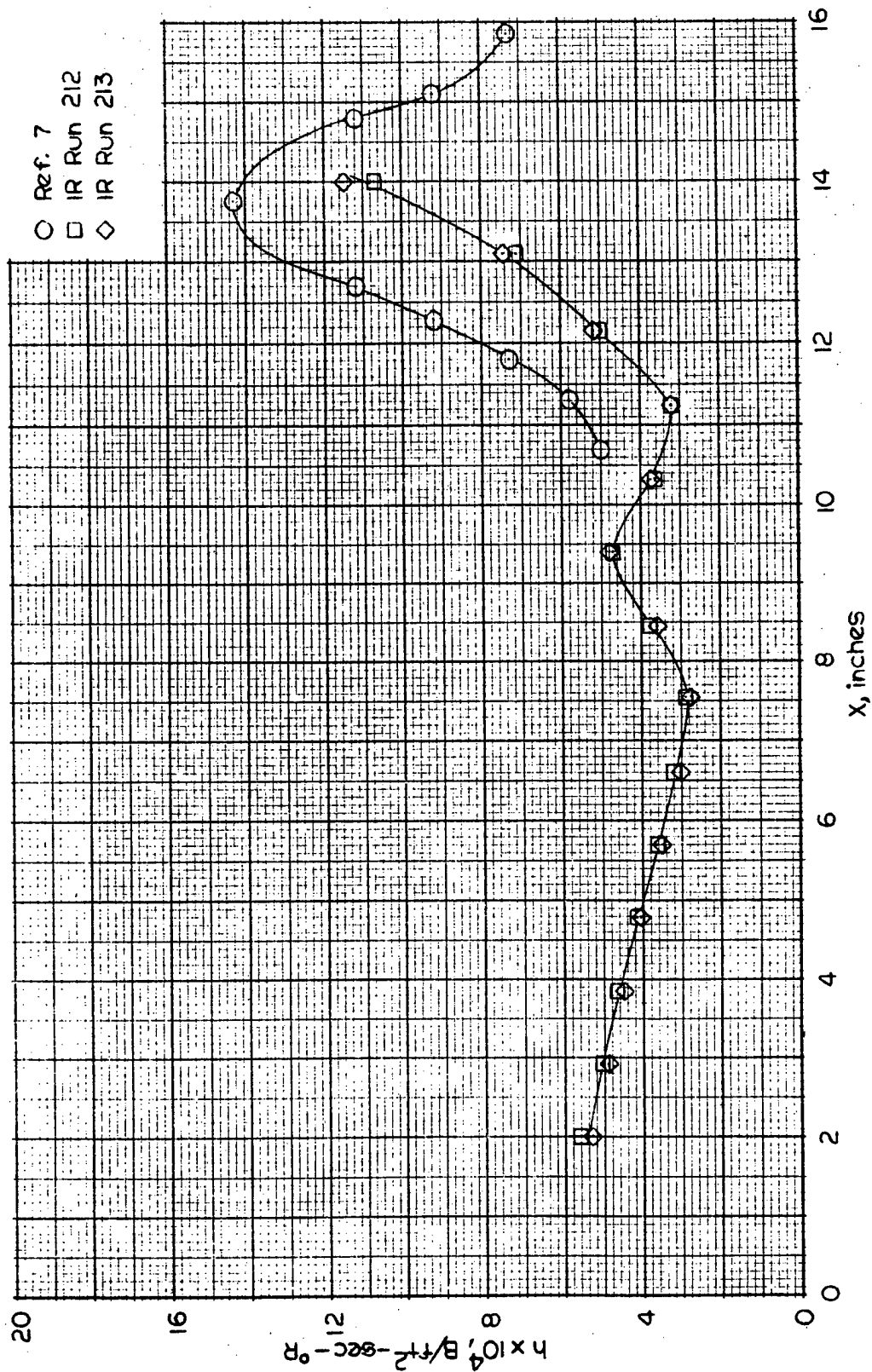
a. $Y = 1.42$ in.

Figure 7. Comparison of Heat Transfer Coefficients for $\lambda_F = 0$ in.,
Scan Angle = -10 deg.



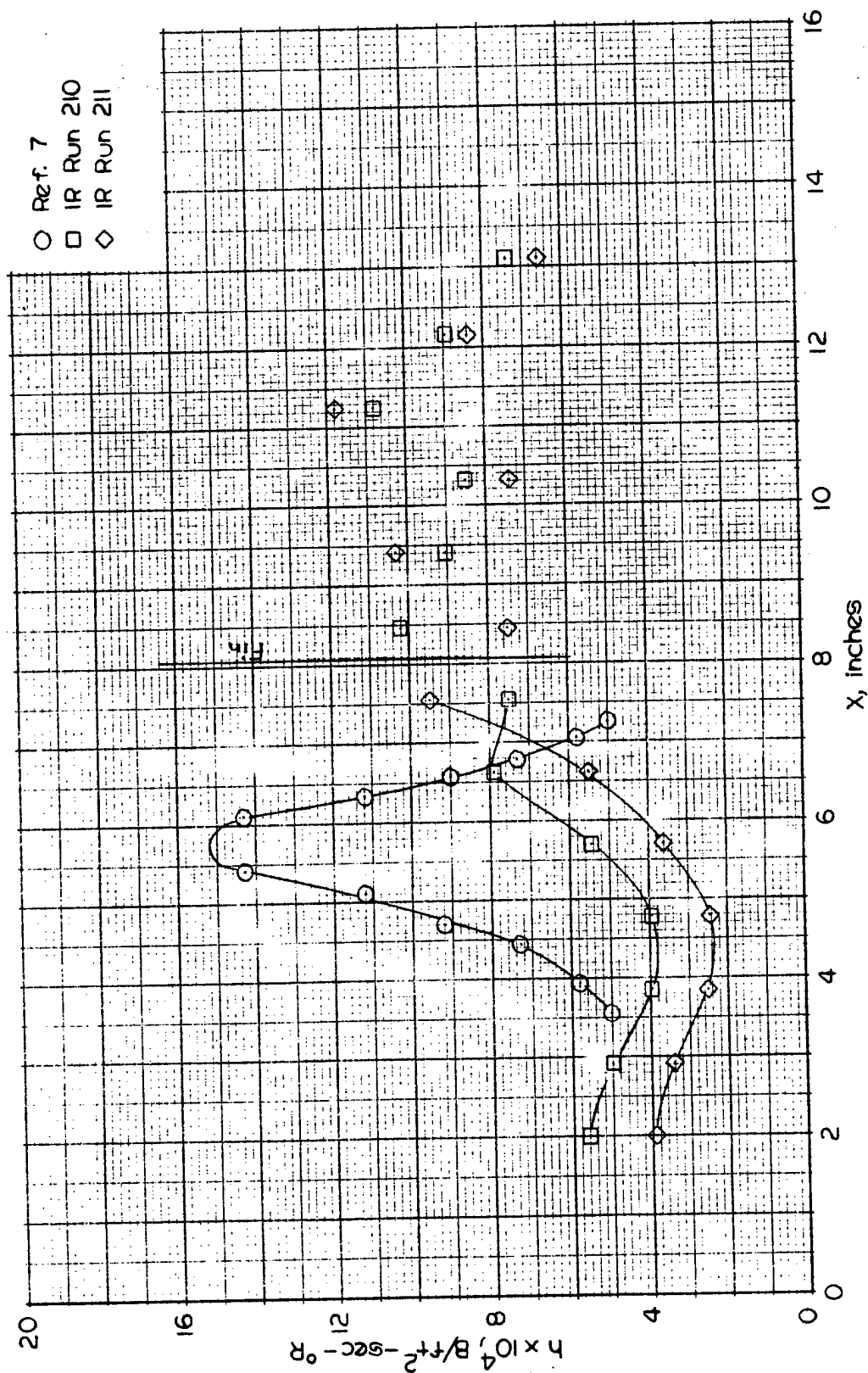
b. $Y = 2.53$ in.

Figure 7. (Continued)



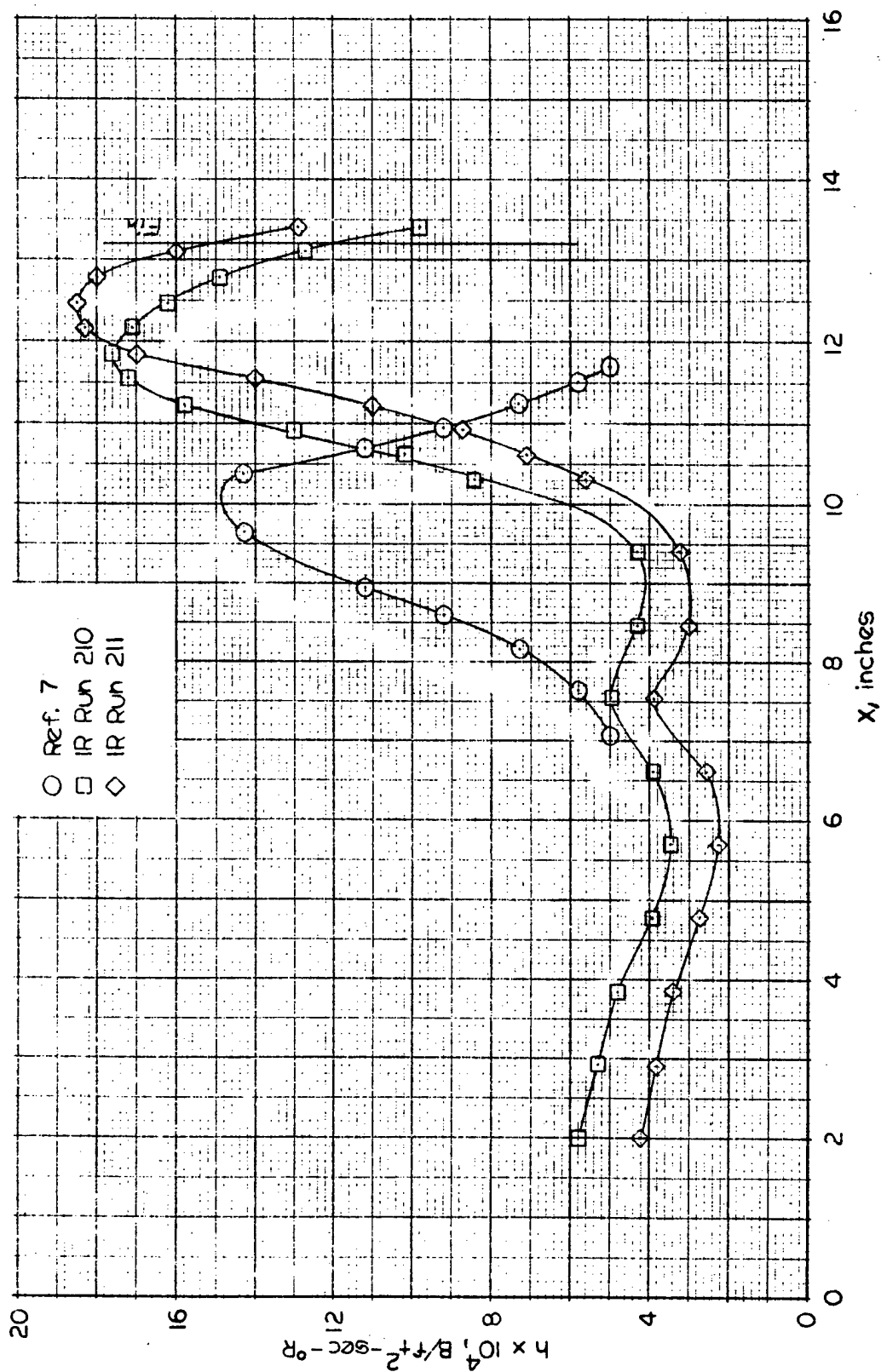
c. $Y = 5.24$ in.

Figure 7. (Concluded)

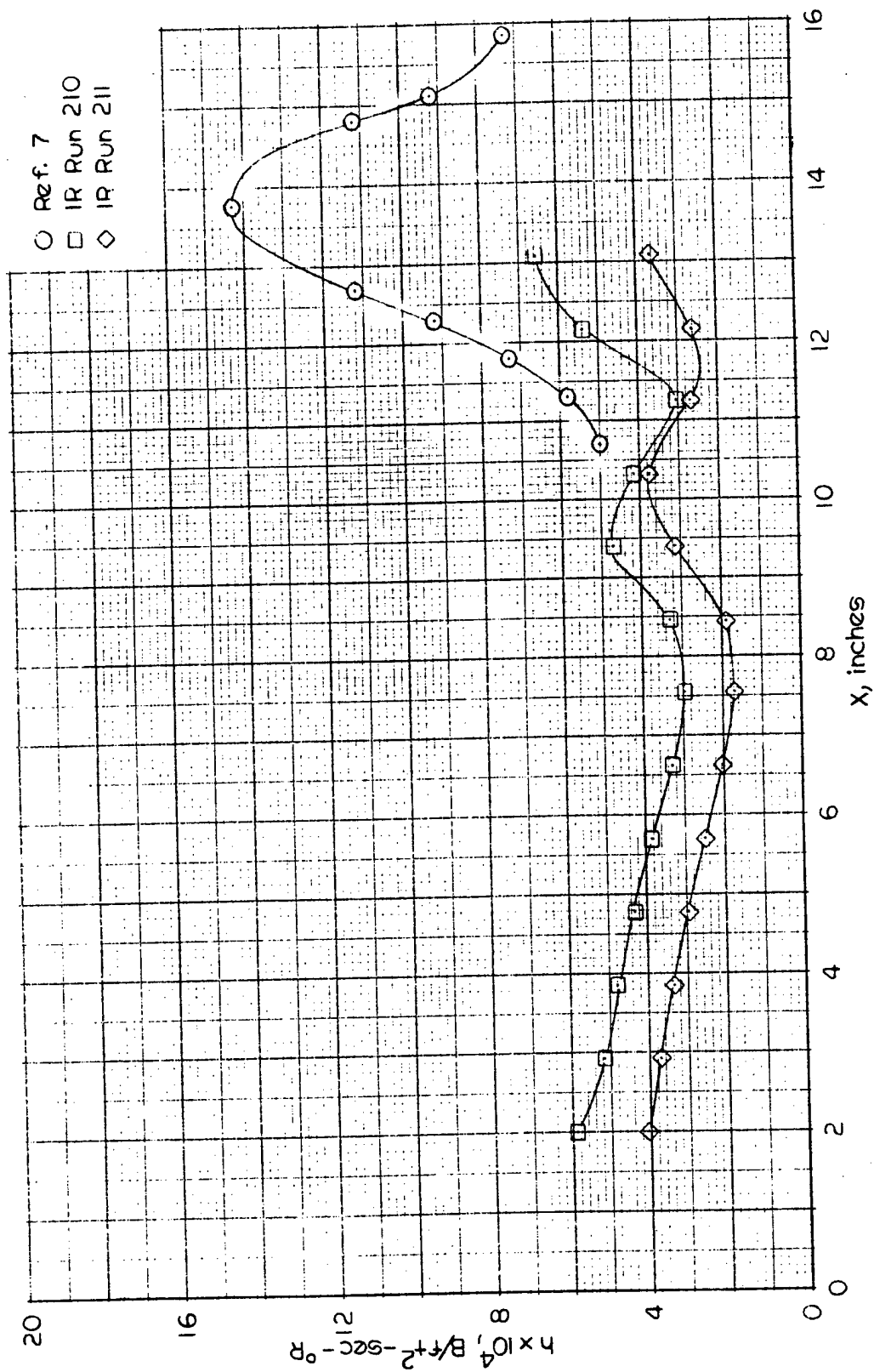


a. $y = 1.12$ in.

Figure 8. Comparison of Heat Transfer Coefficients for $\lambda_p = 0$ in., Scan Angle = -20 deg.

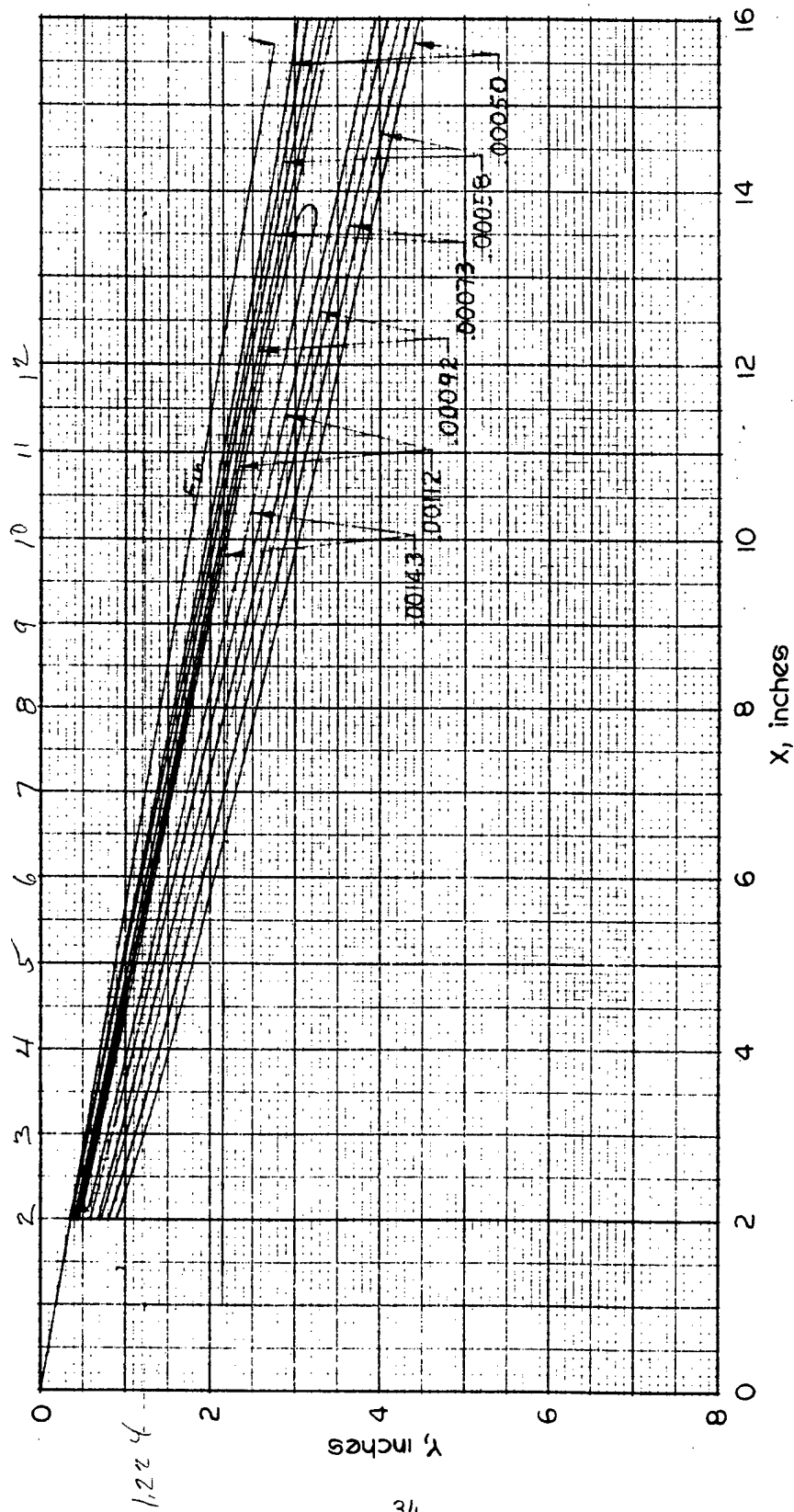


b. $Y = 2.53$ in.
Figure 8. (continued)



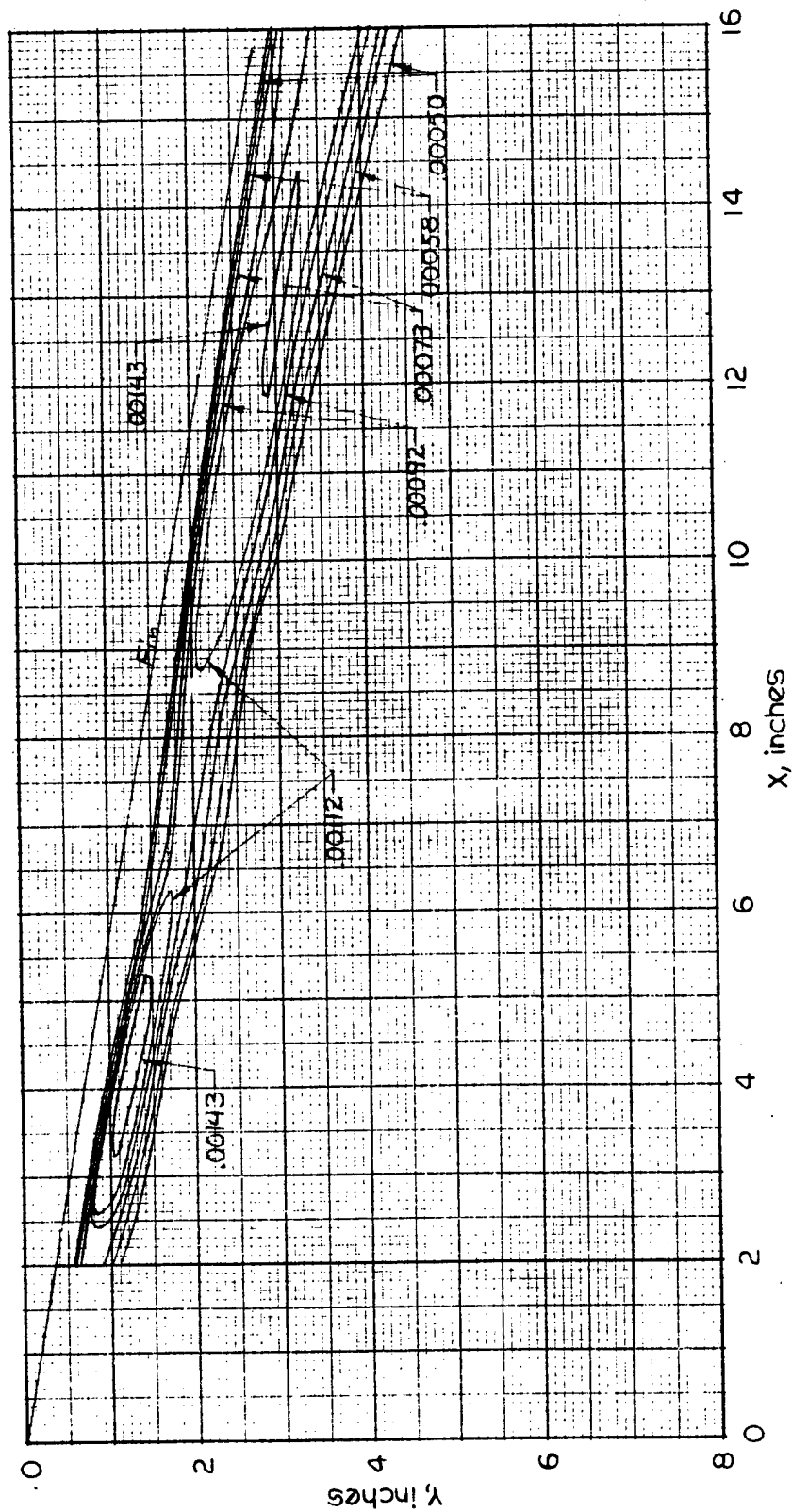
c. Y = 5.24 in.

Figure 8. (Concluded)



a. Reference 7. Run 297

Figure 9. Distribution of Heat Transfer Coefficients



b. IR Scanner Run 199

Figure 9. (concluded)

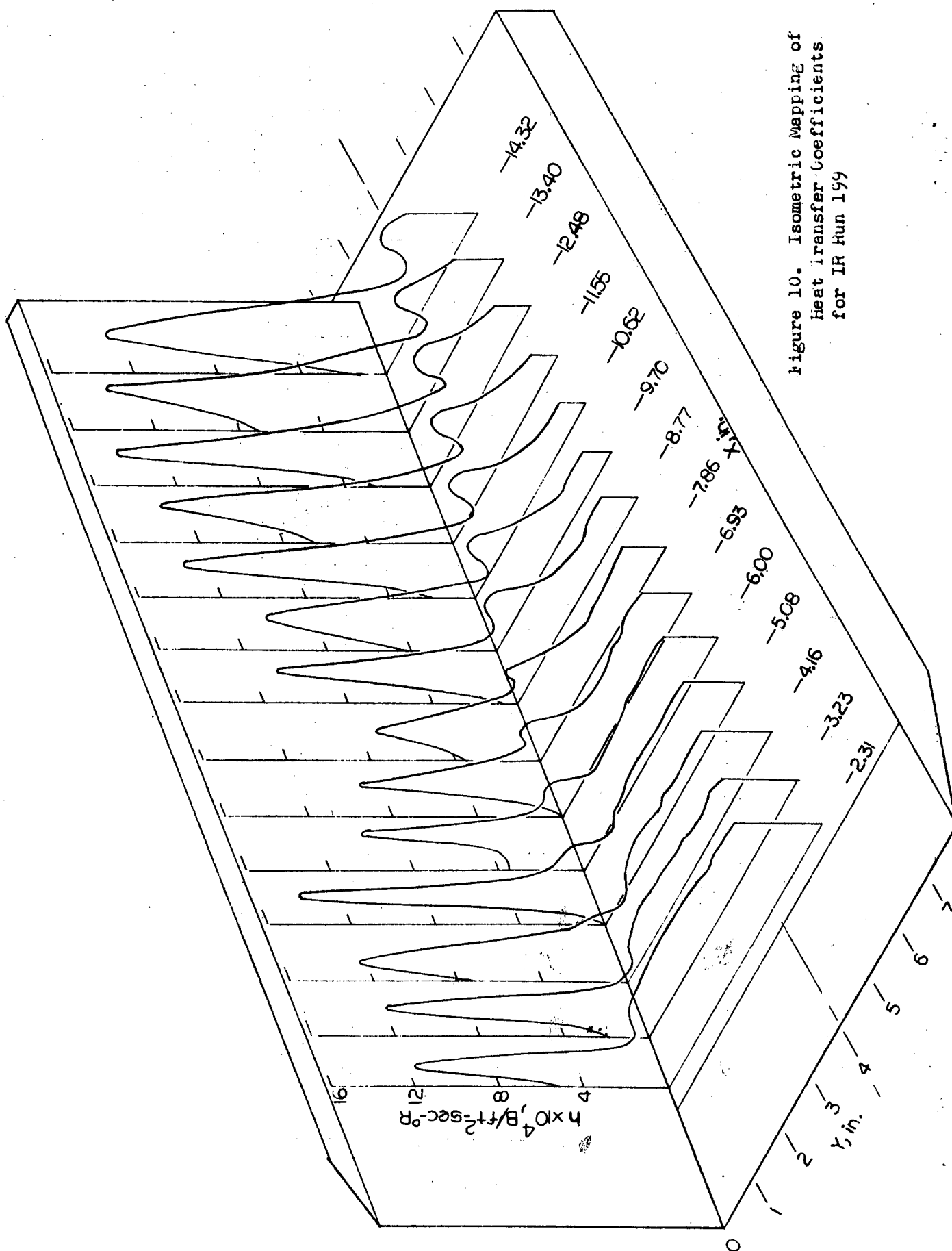


Figure 10. Isometric Mapping of
Heat Transfer Coefficients
for IR Hun 199